3D FEM analysis of earthquake induced pounding responses between asymmetric buildings

Kaiming Bi[*1], Hong Hao[1a] and Zhiguo Sun[2b]

[1]*Center for Infrastructure Monitoring and Protection, School of Civil and Mechanical Engineering,
Curtin University, Kent Street, Bentley, WA 6102, Australia*
[2]*Department of Disaster Prevention Engineering, Institute of Disaster Prevention, Beijing 101601, China*

Abstract. Earthquake-induced pounding damages to building structures were repeatedly observed in many previous major earthquakes. Extensive researches have been carried out in this field. Previous studies mainly focused on the regular shaped buildings and each building was normally simplified as a single-degree-of-freedom (SDOF) system or a multi-degree-of-freedom (MDOF) system by assuming the masses of the building lumped at the floor levels. The researches on the pounding responses between irregular asymmetric buildings are rare. For the asymmetric buildings subjected to earthquake loading, torsional vibration modes of the structures are excited, which in turn may significantly change the structural responses. Moreover, contact element was normally used to consider the pounding phenomenon in previous studies, which may result in inaccurate estimations of the structural responses since this method is based on the point-to-point pounding assumption with the predetermined pounding locations. In reality, poundings may take place between any locations. In other words, the pounding locations cannot be predefined. To more realistically consider the arbitrary poundings between asymmetric structures, detailed three-dimensional (3D) finite element models (FEM) and arbitrary pounding algorithm are necessary. This paper carries out numerical simulations on the pounding responses between a symmetric rectangular-shaped building and an asymmetric L-shaped building by using the explicit finite element code LS-DYNA. The detailed 3D FEMs are developed and arbitrary 3D pounding locations between these two buildings under bi-directional earthquake ground motions are investigated. Special attention is paid to the relative locations of two adjacent buildings. The influences of the left-and-right, fore-and-aft relative locations and separation gap between the two buildings on the pounding responses are systematically investigated.

Keywords: irregular asymmetric building; arbitrary pounding; 3D FEM; torsional responses; relative location

1. Introduction

Earthquake-induced pounding damages between adjacent buildings were repeatedly observed in many previous major earthquakes due to the insufficient separation gap and out-of-phase vibrations of adjacent buildings. For example, it was reported that over 40% of the surveyed buildings experienced certain extent of pounding in the 1985 Mexico City earthquake, and 15% led to structural collapse (Rosenblueth and Meli 1985). Cole *et al.* (2012) reported that 6-12% of the surveyed buildings were observed to have severe damage resulting from pounding in the 2011 Christchurch earthquake. Chouw and Hao (2012) conducted a detailed survey of pounding damages of adjacent buildings immediately after the Christchurch earthquake, and concluded that brittle unreinforced masonry (URM) buildings with large window or door openings are especially vulnerable to poundings; and spatial variation of ground movement due to excessive liquefaction of soil has

a potential to increase the magnitude of relative response between adjacent structures, which are a possible reason of widespread pounding damage in Christchurch. Fig. 1 shows the typical pounding induced damages between adjacent buildings. As shown in Fig. 1(a), localized damage occurred around the colliding area (Hao 2015); Fig. 1(b) shows that significant pounding damage occurred over the whole height of the building interface (Cole *et al.* 2012); Fig. 1(c) shows the pounding between a two-story small building and a three-story large building with a setback of about 5 m, severe damage was observed in the smaller two-story building (Rajaram and Ramancharla 2012).

Extensive research works have been carried out by different researchers on the earthquake-induced pounding responses between adjacent buildings. In those studies, most of them focused on the translational pounding and the buildings were modelled as single-degree-of-freedom (SDOF) systems (Anagnostopoulos 1988, Jing and Young 1991, Davis 1992, Hao *et al.* 2000, Chau and Wei 2001, Chau *et al.* 2003) or simplified multiple-degree-of-freedom (MDOF) systems with the masses of the buildings lumped at the floor levels (Maison and Kasai 1990, Filiatrault *et al.* 1994, Jankowski 2008, Cole *et al.* 2011, Efaimiadou *et al.* 2013a, 2013b). By using these simplified models, the geometrical irregularities of the buildings cannot be realistically considered since each floor of the buildings is

---

*Corresponding author, Senior Lecturer
 E-mail: kaiming.bi@curtin.edu.au
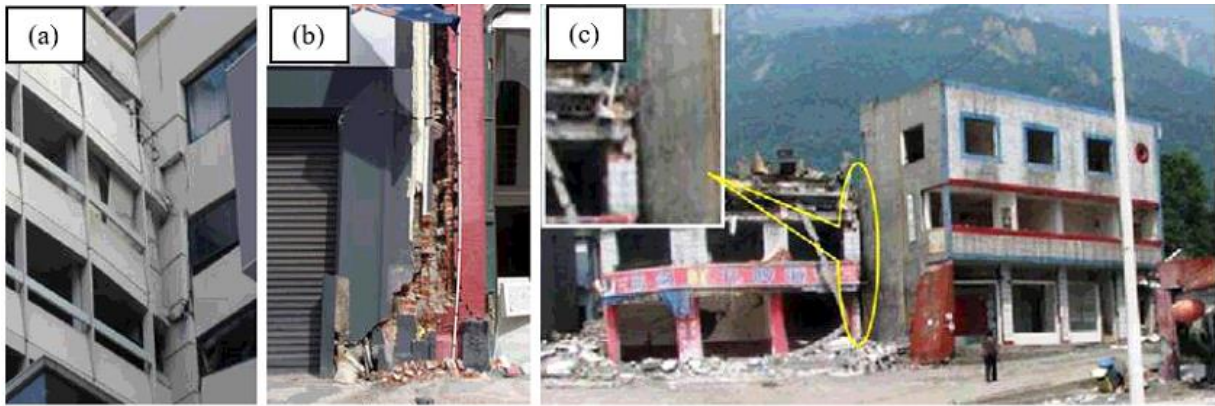[a]Professor
[b]Associate Professor

Fig. 1 Typical earthquake-induced pounding damages between adjacent buildings: (a) and (b) in the 2011 Christchurch earthquake; and (c) in the 2008 Wenchuan earthquake

modelled by a lumped mass, and pounding is assumed occurring between the mass centers of adjacent structures. On the other hand, almost all the buildings in engineering practice are irregular. Any irregularities, eccentricities or asymmetries in plan may result in the torsional responses of buildings when they are subjected to earthquake loading, which in turn may lead to the eccentric poundings between them and thus significantly increase the impact potential. The above simplified models, therefore, may lead to inaccurate estimations of earthquake-induced pounding responses between adjacent buildings. To more realistically simulate the torsional response induced poundings between adjacent building structures, some researchers considered the eccentricities in the building by introducing the center of stiffness (CS) and center of mass (CM) of the each floor not coincident with each other (e.g., Gong and Hao 2005, Hao and Gong 2005, Wang *et al.* 2009 and Fiore *et al.* 2013). Coupled lateral-torsional pounding responses were investigated by considering different impact scenarios. Papadrakakis *et al.* (1996) developed a three-dimension (3D) model to simulate pounding responses between two or more adjacent buildings during earthquakes. The eccentricity was induced by the different stiffness in different supporting columns. Leibovich *et al.* (1996) and Mouzakis and Papadrakakis (2004) investigated the eccentric poundings between two sets of symmetric buildings symmetrically or asymmetrically aligned with respect to each other. It should be noted that though eccentric poundings were considered in the last three studies, the buildings are in symmetric rectangular shapes. To investigate the influence of plan irregularity, Jankowski (2009, 2012) investigated earthquake-induced pounding between the main building and the stairway tower of the Olive View Hospital based on the detailed 3D finite element models (FEM). Numerical results show that the torsional vibrations of the buildings resulting from the asymmetries in plan induce eccentric poundings. More recently, Soltysik and Jankowski (2016) carried out numerical simulations on the pounding responses between two L-shaped asymmetric steel buildings. The results again indicate that torsional vibrations play an important role in the overall pounding-involved responses of asymmetric buildings.

The stereo-mechanical method and the contact element method, were commonly used by different researchers. The stereo-mechanical method assumes the duration of an impact is zero and computes the velocities of each rigid body based on the conventional impulse-momentum law (Goldsmith 1960). This method has clear physical meaning but cannot predict the magnitude of the pounding force and the duration of the collision due to the method's underlying assumption. Many previous studies (e.g., Leibovich *et al.* 1996, Papadrakakis *et al.* 1996, Mouzakis and Papadrakakis 2004) adopted stereo-mechanical method to model pounding. Compared to stereo-mechanical method, contact element method is more commonly used (Favvata 2017, Ghandil and Aldaikh 2017) and almost all the other studies mentioned above used this method to simulate pounding. A contact element uses a spring element, a damping element or their combination in conjunction with a gap element to simulate the impact. Several linear and nonlinear contact models have been developed. Hao *et al.* (2013) provided an extensive review on these models. Contact element method can be easily implemented in the finite element software. The drawback of this method is that a contact element is connected between two nodes, in other words, the pounding locations are predetermined and only the point-to-point pounding can be considered in the simulation.

For building structures subjected to seismic loading, pounding might take place along the entire surface of adjacent structures. Moreover, due to the irregularities of the structures, eccentric poundings are more prone to occur compared to the translational poundings. The pounding locations therefore could not be predetermined. In this case, the contact element method which based on the point-to-point pounding assumption may not be able to give accurate estimations of pounding responses especially considering the fact that eccentric poundings are unavoidable. To overcome this limitation, Zhu *et al.* (2002) and Guo *et al.* (2011) proposed 3D contact-friction models to simulate the arbitrary pounding between adjacent structures. Gong and Hao (2005) and Hao and Gong (2005) developed a program to search the pounding location between two adjacent buildings at each time step during the solution of dynamic responses and calculated the torsional responses of adjacent structures induced by eccentric poundings. Polycarpou *et al.* (2014) presented a numerical approach to consider the

pounding response between multistory buildings. The proposed method has no limitations regarding the geometry of the structures and their positions in plan. It should be noted that these methods are not readily available in the commercial software, which limits their applications. More recently, Bi and his colleagues (Bi *et al.* 2013, Bi and Hao 2013, 2015, He *et al.* 2016) investigated the arbitrary pounding responses between different components of bridge structures by using the commercial software LS-DYNA based on the detailed 3D FEM. The accuracy of the method was validated by comparing the numerical results with the analytical solution (Bi *et al.* 2013) and experimental data (He *et al.* 2016). It was found that this method can conveniently simulate the possible point-to-point, point-to-surface and surface-to-surface poundings without the necessity to predefine the pounding locations (Bi and Hao 2013, 2015). This method therefore yields most realistic simulations of arbitrary 3D poundings. However, to the best knowledge of the authors, this method has never been applied to simulate the pounding responses between adjacent buildings.

Critical literature review reveals that previous studies on earthquake-induced pounding responses between adjacent buildings mainly focused on the regular shaped structures based on the lumped mass models. The researches on the pounding responses between irregular asymmetric buildings, where torsional vibrations of the structures may play a significant role, are rare. Moreover, pounding phenomenon was normally considered by the contact element method, which is based on the point-to-point pounding assumption with the predetermined pounding locations. This simplification may not be able to realistically consider the actual arbitrary 3D poundings. This paper carries out numerical simulations on the pounding responses between a symmetric rectangular-shaped building and an asymmetric L-shaped building by using the explicit finite element code LS-DYNA. The detailed 3D FEM of the buildings are developed and the arbitrary 3D poundings are considered. Special attention is paid to the relative locations of the two adjacent buildings. The influences of the left-and-right, fore-and-aft relative locations and separation gap between the two adjacent buildings (see Fig. 6) on the pounding responses are systematically investigated. It should be noted soil-structure-interaction (e.g., Mahmoud *et al.* 2013) and ground motion spatial variations (e.g. Hao, *et al.* 2000, Chouw and Hao 2012, Jankowski 2012) can further influence the pounding responses between adjacent buildings. Not to further complicate the problem, the influences of SSI and ground motion spatial variations are not considered in the present study. Moreover, by using the explicit software LS-DYNA, pounding induced damages to the buildings can be considered (Bi and Hao 2013, 2015). This is, however, out of the scope of present study.

2. Building models

2.1 Building information

Fig. 2 shows the considered two adjacent buildings. Each building has three stories with the same story
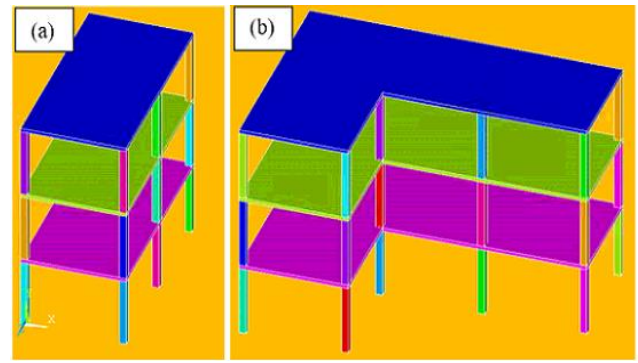

Fig. 2 Two adjacent buildings: (a) Building A and (b) Building B

height. Building A is a symmetric rectangular-shaped building, while Building B is an asymmetric L-shaped building. Building A has one bay along the *x* direction and two bays along the *z* direction. For Building B, three bays exist in the *x* direction and there are two bays in the *z* direction. The bay lengths in the *x* and *z* directions are the same for both buildings, with a length of 4.5 m. The dimensions of all columns are 0.3×0.3 m and the height of each column is 3 m. The floor slab is 0.15 m thick. The Young's modulus and density of the columns and slabs are 3.0×10^{10} Pa and 2400 kg/m^3, respectively. The longitudinal reinforcement ratio for the column is 1.2% and that for the slab is 1%. For Building B, a live load of 3 kN/m^2 is applied on each floor. Based on descriptions above, it is obvious that poundings will occur at the story levels.

2.2 FE models and vibration characteristics

The FE models of the two buildings are developed by using the finite element code ANSYS and the analyses are carried out in LS-DYNA. Convergence test shows that a size of 0.15 m for all the building components can yield a good balance between the computational effort and accuracy, the mesh size of 0.15 m is therefore adopted in the numerical models. It should be noted that pounding induced damages to the buildings are not considered in the present study as mentioned above. Smaller mesh size is needed if local damages are of interest.

The smeared RC material, which assumes reinforcement uniformly distributed over concrete element, is used to model all the components of the two buildings. *MAT PSEUDO TENSOR (MAT_16) in LS-DYNA is used to model the smeared material. The advantage of this material model is that it can model the complex behavior of concrete by specifying the unconfined compressive strength only when no detailed concrete material experiment data is available. In the present study, the unconfined compressive strength of the concrete is 30 MPa. This model can significantly reduce the computational effort compared to modelling the concrete and reinforcement separately.

The penalty method approach is adopted to model the contact interfaces between meshes because of its effectiveness and simplicity for explicit analysis. With this method slave nodes penetration is restricted via the

(a) T_{A1}= T_{Ax}=0.5199 s   (b) T_{A2}= T_{Az}=0.5147 s   (c) T_{A3}= $T_{A\theta}$=0.3716 s

(d) T_{B1}= T_{Bz}=0.7032 s   (e) T_{B2}= T_{Bx}=0.6984 s   (f) T_{B3}= $T_{B\theta}$=0.5691 s
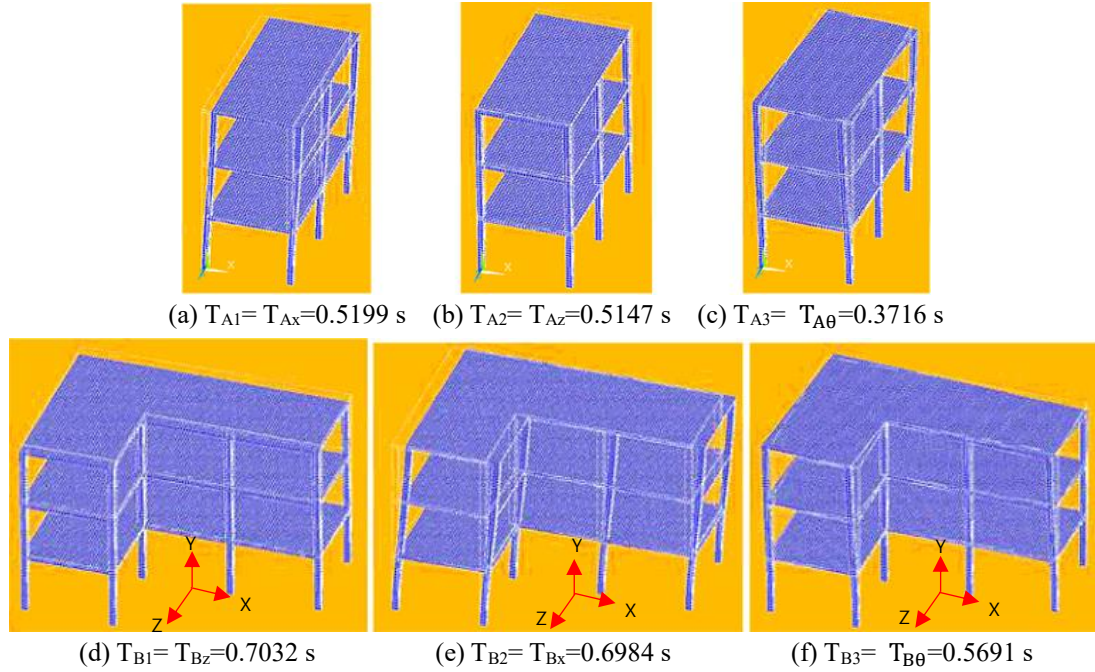
Fig. 3 First three vibration periods and corresponding vibration modes for the two buildings: (a)-(c) Building A and (d)-(f) Building B
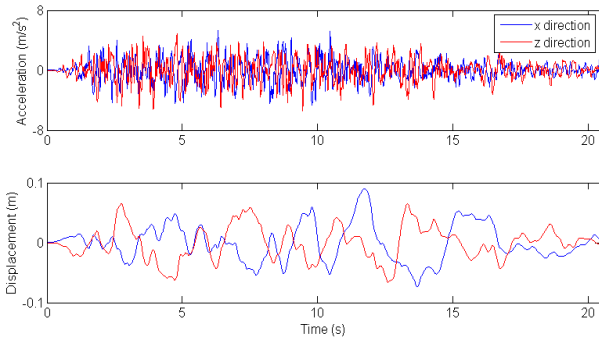

Fig. 4 Simulated acceleration and displacement time histories in the *x* and *z* directions
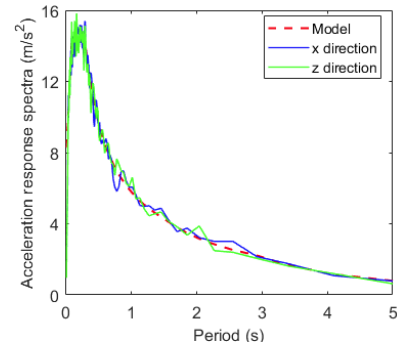

Fig. 5 Comparison of the simulated and target response spectra

imaginary normal interface springs between the shooting nodes and contact surface. The contact algorithm of *CONTACT AUTOMATIC SURFACE TO SURFACE in LS-DYNA is employed to model the potential 3D arbitrary poundings between adjacent buildings. The static and dynamic Coulomb friction coefficients need to be defined in the simulation, and they are set to be 0.5 in this study (Jankowski 2009, 2012).

With the detailed information mentioned above, the dynamic properties of the two buildings can be estimated by carrying out an eigenvalue analysis. Fig. 3 shows the first three vibration frequencies and the corresponding vibration modes of the two buildings. To more clearly show the directions of vibration modes, the un-deformed edge of the structures are also shown in the figures (the white lines). As shown in Figs. 3(a)-(c), the first three vibration periods for Building A are 0.5199, 0.5147 and 0.3716 s respectively in the longitudinal (*x*), transverse (*z*) and torsional (*θ*) directions. For Building B, the first three vibration periods are 0.7032, 0.6984, 0.5691 s for the transverse (*z*),

longitudinal (*x*) and torsional (*θ*) directions, respectively as shown in Figs. 3(d)-(f). Normally, the torsional to longitudinal vibration frequency ratio f_θ/f_x is used to define whether the system is torsinally stiff or torsionally flexible (Gong and Hao 2005). When the ratio f_θ/f_x is less than 1.0, the system is torsionally flexible and the torsional vibration mode is easier to be excited than the translational responses, vice versa. In the present study, $f_{A\theta}/f_{Ax} = 1.399$ and it is larger than $f_{B\theta}/f_{Bx} = 1.227$. Both building models are torsionally stiff, and therefore translational responses will be easier to be excited. Regarding the torsional responses, torsional vibration mode of Building B is easier to be excited than that of Building A.

3. Earthquake loadings

Bi-directional earthquake loadings in the *x* and *z* directions are stochastically simulated based on the spectral representation method proposed by Bi and Hao (2011).

These two ground motion time histories are generated to be compatible with the design spectrum for shallow soil site (Class C) specified in the New Zealand Seismic Loading Code. In the simulation, the ground motions in the two directions are assumed to be stochastically independent of each other, the peak ground acceleration (PGA) is set as 0.5 g and the time duration is 20.47 s, the sampling frequency and upper cut off frequency are 100 and 25 Hz, respectively. Fig. 4 shows the simulated acceleration and displacement time histories in the x and z directions respectively and Fig. 5 compares the response spectra of the generated time histories and the given model, good match is observed as shown.

4. Numerical results

The pounding responses between two adjacent buildings with different relative locations are investigated in this section based on the detailed 3D model with the consideration of possible 3D poundings. The accuracy of the method has been validated in many previous studies (e.g., Bi *et al.* 2013, Bi and Hao 2013, 2015), and previous studies indicated that the detailed 3D model can more realistically consider the surface-to-surface and torsional response induced eccentric poundings compared to the simplified 1D and 2D models. For conciseness, the validation of the method is not reported in the present study, interested readers can refer to the fore mentioned previous studies.

Fig. 6 shows the relative locations between the two adjacent buildings considered in the study. Building A is on the left of Building B in Fig. 6(a), while in Fig. 6(b) Building A is on the right of Building B. Fig. 6(c) shows two buildings with a setback S and Fig. 6(d) shows two buildings with a separation gap G. Table 1 tabulates different cases investigated in the present study. For comparison, the case without pounding (Case 1) is also considered in the present study. It should be noted that since interactions are not considered in the non-pounding case, the seismic responses of the both buildings are therefore not influenced by their relative locations.
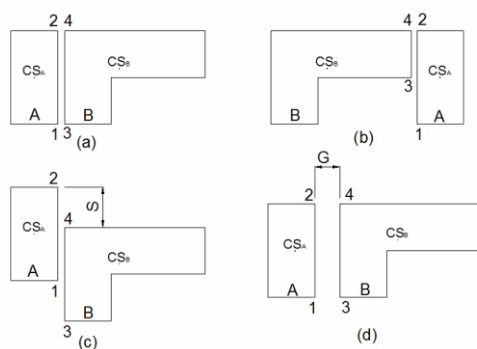

Fig. 6 Different relative locations between two adjacent buildings: (a) Building A is on the left of Building B, (b) Building A is on the right of Building B, (c) Buildings A and B with a setback S and (d) Buildings A and B with different a separation gap G

Table 1 Different cases

Cases	Arrangement	Setback S (m)	Separation gap G (m)	With/without pounding
1	Fig. 6(a)	0	NA	Without
2	Fig. 6(a)	0	0.05	With
3	Fig. 6(b)	0	0.05	With
4	Fig. 6(c)	4.50*	0.05	With
5	Fig. 6(c)	2.25	0.05	With
6	Fig. 6(c)	-2.25	0.05	With
7	Fig. 6(c)	-4.50	0.05	With
8	Fig. 6(d)	0	0.001	With
9	Fig. 6(d)	0	0.1	With

*Positive S means Building A is on the left top of Building B (the one shown in Fig. 6(c))
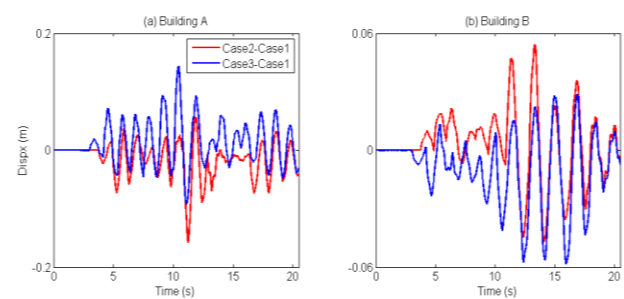

Fig. 7 Influence of left-and-right relative location on the pounding induced longitudinal displacements

It is obvious that the responses at the top story (level three in Fig. 3) will be the largest compared to those at the bottom stories. For conciseness, only the results at the top story are presented in the following sections. Particularly the results at the stiffness centers (CS_A and CS_B) and points 1-4 shown in Fig. 6 are discussed.

4.1 Influence of left and right relative location (Figs. 6(a) and 6(b))

The influence of left-and-right relative location is firstly investigated. In these two cases (Cases 2 and 3), the setback S is 0, and the separation gap between the two buildings is G=0.05 m.

To demonstrate the influence of pounding more clearly, the (absolute) displacements obtained at the stiffness centers of the two buildings from the pounding cases (Cases 2 and 3) are subtracted by the corresponding results without consideration of pounding (Cases 1). Fig. 7 shows the pounding induced longitudinal displacements for the two arrangements. As shown, when Building A locates on the left of Building B (Case 2), pounding induced maximum displacement is about 0.157 m for Building A. For Building B, the maximum displacement is about 0.056 m. As for Case 3, the values are 0.143 and 0.057 m respectively for Buildings A and B. For the both arrangements, the influence of pounding on Building A is much more evident than Building B. This is because the mass of Building A is 43.74 ton, which is much lighter than that of Building B (160.38 ton). These results are consistent with previous studies (e.g.,
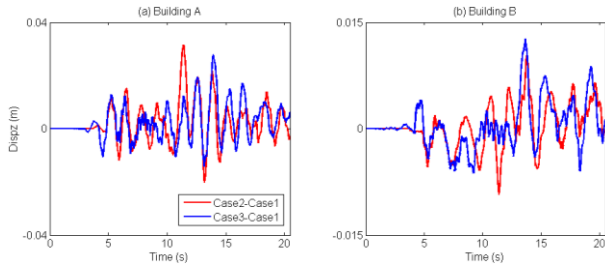
Fig. 8 Influence of left-and-right relative location on the pounding induced transverse displacements

Fig. 10 Influence of left-and-right relative location on the torsional responses of two buildings
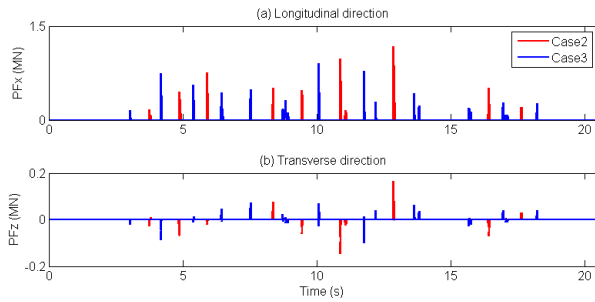

Fig. 9 Pounding force time histories in the longitudinal and transverse directions with different left-and-right relative locations

Gong and Hao 2005, Jankowski 2008, 2009), in which they indicated that the responses of a lighter structure can be substantially influenced by the structural interactions. Fig. 7 also shows that left-and-right relative location of the two buildings can obviously influence the longitudinal displacements of the two buildings. However, there is no obvious trend between the arrangement and pounding induced longitudinal displacement, and its influence on the maximum longitudinal displacement is not evident as can be seen from the results above.

Fig. 8 shows the pounding induced transverse displacements (*z* direction in Fig. 3) for the two cases. Similar to the responses in the longitudinal direction, the influence of pounding on Building A is more evident than Building B due to different masses of the two buildings. The arrangement scenarios between the two buildings can influence the pounding induced transverse displacement but again its influence on the maximum response is not evident.

Left-and-right relative locations of the two buildings can obviously change the interactions between them. Fig. 9 shows the pounding forces between the two buildings at level three in the longitudinal and transverse directions. As shown, when Building A is located on the left of Building B, 10 poundings occur between these two buildings. For Case 3, 16 poundings occur. This is because for Case 3, poundings occur between the top parts of two buildings and these eccentric poundings further exaggerate the torsional responses of both buildings (detailed results can be seen from Fig. 10), which makes the two building more prone to pounding. On the other hand, the maximum pounding forces in Case 2 are larger than those in Case 3. As shown in Fig. 9(a), the maximum pounding forces in the longitudinal direction are 1.17 and 0.91 MN respectively for Cases 2 and 3, and the values in the transverse directions
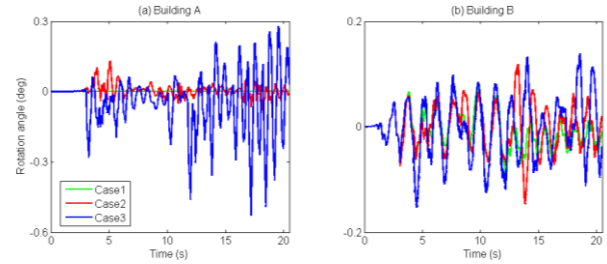
are 0.167 and 0.099 MN respectively. This is because poundings tend to occur along the entire contacting areas between the two buildings in Case 2, and therefore more mass contributes to pounding.

The torsional responses of the two buildings can be estimated by the rotational angles between points 1 and 2 for Building A and between points 3 and 4 for Buildings B (Fig. 6). These can be achieved by dividing the relative longitudinal displacements between these points by the corresponding distances between them, which are 9 and 4.5 m respectively as shown in Fig. 6. Fig. 10 shows the numerical results. As shown in Fig. 10(a), no rotational angle is observed for Building A when pounding is not considered (green curve) because it is a symmetric building. However, for Building B, obvious rotational response can be obtained even though pounding is not considered. This is actually expected: Building A is in a symmetric rectangular shape, the mass center and stiffness center coincide with each other, therefore no torsional response can be excited under the translational earthquake loadings. While Building B is an asymmetric L-shaped building, the mass center and stiffness center do not coincide, torsional response will therefore be excited under the translational earthquake loadings.

Pounding obviously amplifies the torsional responses of Building A and the amplification is more evident in Case 3 compared to that in Case 2. As shown in Fig. 10(a), the maximum rotational angles are 0.13 and 0.52 degrees for Cases 2 and 3 respectively. This is because pounding forces only act at the top part of Building A in Case 3 as mentioned above, which may result in the rigid body rotation in the building because of the eccentric pounding forces. While for Case 2 poundings tend to act along the whole surface and Building A tends to move translationally, which in turn results in smaller rotational response. For Building B (Fig. 10(b)), pounding slightly amplifies the torsional responses but with less extent compared to Building A because Building B is much heavier. The arrangement of Case 3 leads to slightly larger rotational angle most of the time compared to Case 2. This is again can be explained by the eccentric poundings as mentioned above.

The numerical results indicate that for the two arrangements, pounding will induce almost the same extent of longitudinal and transverse displacements to the two buildings. However, the arrangement in Case 3 leads to much larger torsional response especially to the lighter building, which in turn results in worse performance of the
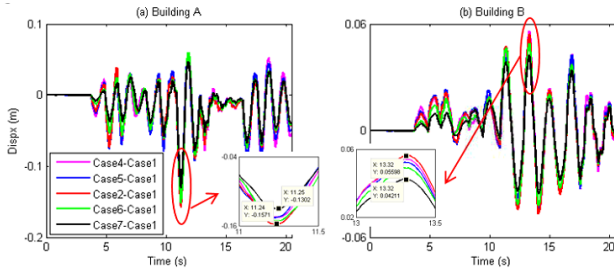
Fig. 11 Influence of setback on the pounding induced longitudinal displacements of two buildings

Fig. 12 Influence of setback on the pounding induced transverse displacements of two buildings

building during a severe earthquake. The arrangement in Case 3 should be avoided in the design in terms of preventing pounding induced damages to building structures. It should be noted that if each floor of the two buildings is modelled by the simplified lumped mass model as adopted in many previous studies, the left-and-right relative location of the two buildings will not influence the structural responses. These results, on the other hand, show that the detailed 3D modelling can result in more accurate structural response estimations compared to the simplified model.

4.2 Influence of fore-and-aft relative location (setback)

This section investigates the influence of fore-and-aft relative location (setback) on the pounding responses between these two buildings. Only the arrangement shown in Fig. 6(c), i.e., Building A locating on the left of Building B, is considered. Five different setbacks are investigated with S=4.50 (Case 4), 2.25 (Case 5), 0 (Case 2), -2.25 (Case 6) and -4.50 m (Case 7), respectively. The separation gap is G=0.05 m.

Only the pounding induced displacements are taken out for analyses again. Figs. 11 and 12 show the pounding induced longitudinal and transverse displacements respectively. Similar to those obtained in Figs. 7 and 8, the influence of pounding on the lighter Building A is more evident than that on the heavier Building B. As shown in Fig. 11, the influence of setback on the pounding induced longitudinal displacements of two buildings is not prominent. The case without setback (Case 2) leads to the largest difference with 0.157 m for Building A and 0.056 m for Building B as shown in the enlarged figures. Generally speaking, increasing setback results in less difference. As shown, the smallest differences are 0.130 m and 0.042 m respectively for Buildings A and B, and they occur in the case with a setback of -4.50 m (Case 7). This is because the contacting portions decrease with the increment of setback and less mass contributes to pounding as shown in Fig. 6. The results also show that with the same setback of 4.50 m (Cases 4 and 7), Case 7 leads to smaller differences compared to Case 4. This is because the mass of Building B mainly concentrates at the top part of the building, more mass contributes to pounding in Case 4.

The influence of setback on the pounding induced transverse displacement is not evident as shown in Fig. 12. Different setbacks lead to almost the same transverse
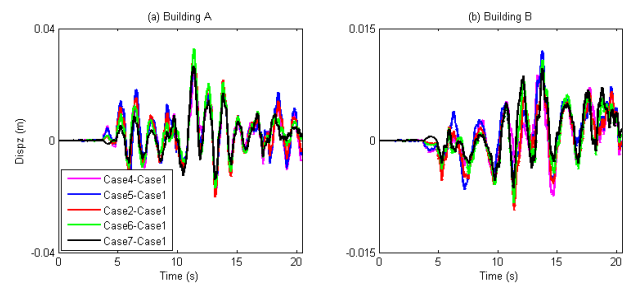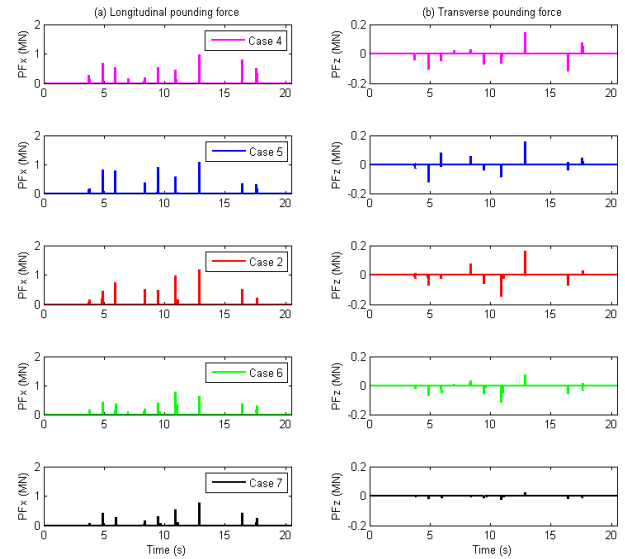

Fig. 13 Pounding force time histories between two buildings with different setbacks

displacements. Elaborative analyses reveal that similar to the longitudinal displacement, Cases 4 and 7 generally lead to the smallest difference. Namely when the setback is large, the influence of pounding on the transverse displacement is less evident compared to the smaller setback.

Fig. 13 shows the influence of setback on the pounding force. It can be seen that increasing setback leads to smaller pounding forces both in the longitudinal and transverse directions. As shown in Fig. 13(a), the maximum longitudinal pounding forces are 0.981 (Case 4), 1.070 (Case 5), 1.170 (Case 2), 0.776 (Case 6) and 0.768 MN (Case 7) respectively. For the transverse pounding force, the maximum values are 0.147, 0.158, 0.165, 0.115 and 0.025 MN respectively. This is again can be explained by the mass contribution. When there is no setback, the whole mass of the two buildings contribute to pounding, while less mass contributes to pounding with the increment of setback. With the same setback, Case 4 causes larger pounding force than Case 7 due to the reason mentioned above.

Fig. 14 shows the influence of setback on the rotational angles of the two buildings. As shown, the influence of setback on Building A is more significant compared to Building B. Moreover, the larger is the setback, the more likely will the eccentric poundings occur and the larger is the rotational angle for both buildings. As shown in Fig.
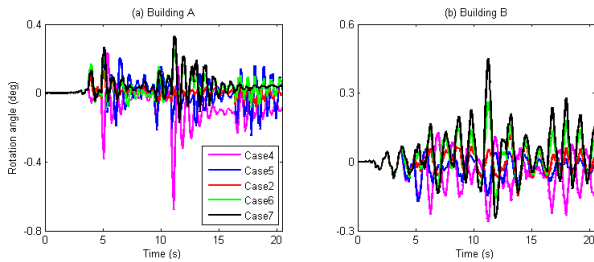
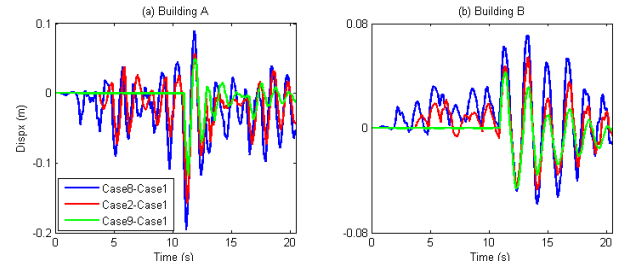Fig. 14 Influence of setback on the torsional responses of two buildings

Fig. 15 Influence of separation gap on the pounding induced longitudinal displacements of two buildings

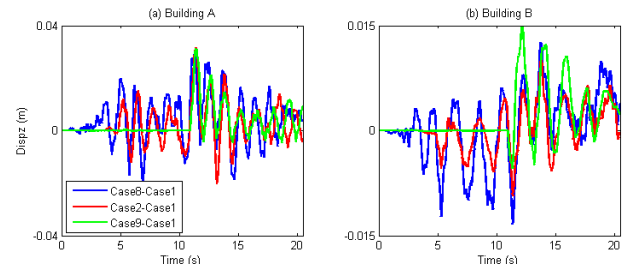Fig. 16 Influence of separation gap on the pounding induced transverse displacements of two buildings

14(a), the largest rotational angle reaches 0.670 degree in Case 4 (S=4.50 m), while in Case 2 (S=0 m), the maximum rotational angle is only 0.130 degree. For Building B, as shown in Fig. 14(b), the largest rotational angle of 0.450 degree occurs in Case 7 with a setback of -4.50 m. For the case without setback, the maximum rotational angle is 0.147 degree. It also can be seen that with the same setback of 4.50 m, Case 4 leads to much larger rotational angle compared to Case 7 for Building A. This is because as shown in Table 1, pounding locations for Building A is more or less the same compared to the stiffness center in these two cases (the difference is that poundings occur at the bottom part in Case 4 and at the top portion in Case 7). However, pounding forces in Case 4 are larger than those in Case 7 as shown in Fig. 13, which in turns leads to the larger rotational angle. For Building B, opposite results are obtained, namely Case 7 leads to larger rotational angle compared to Case 4. This is because poundings occur at the bottom part of Building B in Case 7 and they occur on the top part on in Case 4 as shown in Table 1. Pounding in Case 4 mainly leads to the translational vibration of Building A since pounding locations are close to the stiffness center of the building though the pounding force in Case 4 is larger. While for Case 7, pounding force acting location is far from the stiffness center of Building B, which means eccentric poundings dominate the structural response.

The numerical results well explain the reason why the smaller building shown in Fig. 1(c) suffered serious damage while the larger building was almost intact: the large setback results in large torsional responses in the smaller building. The results also indicate that large setback should be avoided in the design in order to mitigate pounding induced torsional responses in the buildings.

4.3 Influence of separation gap (Fig. 6(d))

Separation gap is another parameter which may significantly influence the pounding responses between adjacent structures. Three different separation gaps are considered in this section, i.e. a very small gap with G=0.001 m (Case 8), a medium gap G=0.05 m (Case 2) and a relatively large gap G=0.1 m (Case 9). Again the lighter Building A is assumed locating on the left of heavier Building B, and no setback is considered, i.e., S=0 m.

Figs. 15 and 16 show the influence of separation gap on the pounding induced longitudinal and transverse displacements. Again pounding has more obvious influences on the lighter Building A by comparing the

results in Figs. 15(a) and (b). Fig. 15(a) shows that increasing separation gap leads to smaller difference on the longitudinal displacements for both buildings. As shown, the maximum differences are 0.193 (Case 8), 0.157 (Case 2) and 0.118 m (Case 9) respectively for Building A. While for Building B, the corresponding values are 0.068, 0.056 and 0.045 m respectively. This is expected since larger separation gap means less interactions between the two buildings and the responses of the two buildings are therefore more similar to the non-pounding case.

For the transverse displacement, a similar trend can generally be obtained especially when the separation gap is relatively small (Cases 8 and 2). As shown, the differences with the very small gap (blue curve) are generally larger than those with a medium separation gap (red curve) due to more interactions. However, when the separation gap reaches 0.1 m (Case 9), a slightly different trend is obtained. As shown, largest differences are obtained around 11.4 s for Building A and around 12 s for Building B. This is because an obvious pounding occurs around 10.95 s in Case 9 as shown in Fig. 17. Pounding significantly changes the vibration behaviors of two buildings, which in turn results in the largest differences in Fig. 16. It also can be seen that, the largest differences do not appear at the time when pounding occurs but with slight delay. This is because the structures need time to response. The results are consistent with the results obtained by Jankowski (2008), in which it was indicated that the maximum transverse displacement varies with the separation gap, and no monotonous trend can be obtained.

Fig. 17 shows the influence of separation gap on the longitudinal and transverse pounding forces. As expected, less number of pounding occurs when the separation gap becomes larger. In this study, 15, 10 and 4 poundings occur for the three different cases. The maximum pounding force, however, increases with the increment of separation gap. As
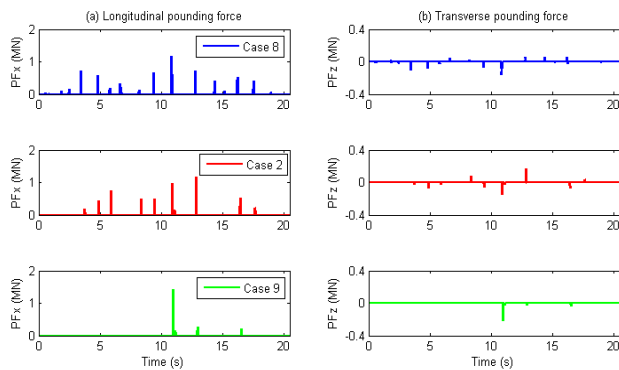
Fig. 17 Pounding force time histories between two buildings with different separation gaps
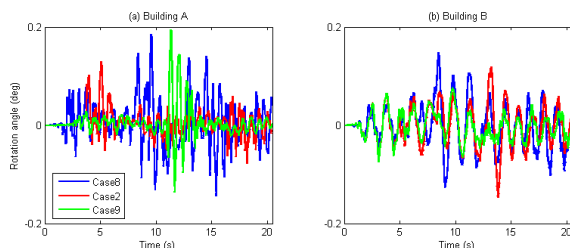

Fig. 18 Influence of separation gap on the torsional responses of two buildings

shown in Fig. 17(a), the maximum longitudinal pounding forces are 1.16, 1.17 and 1.43 MN respectively. As for the maximum transverse pounding force shown in Fig. 17(b), the corresponding values are 0.157, 0.165 and 0.212 MN respectively.

Fig. 18 shows the influence of separation gap on the rotational angles of two buildings. It can be seen that for most of the time Case 8 results in the largest rotational angle and Case 9 leads to the smallest rotational angle. In other words, general speaking smaller separation gap leads to larger rotational angle. However, it also can be seen that, rotational angle is obviously influenced by the pounding. A typical example is Case 9, the pounding occurring at 10.95 s leads to the larger rotational angles of Building A between 11.4 and 12.7 s.

5. Conclusions

This paper carries out numerical simulations on the pounding responses between a symmetric rectangular building and an asymmetric L-shaped building based on the detailed 3D FEM. The arbitrary 3D poundings between the two adjacent buildings are considered. Special attention is paid to the influence of relative locations between the two buildings on the pounding responses. Numerical results show that the lighter building can be significantly influenced by pounding while the influence of pounding on the heavier building is less evident. Particularly, parametric studies reveal that:

• For the asymmetric buildings, left-and-right relative location results in almost the same extent of pounding induced longitudinal and transverse displacements.

However, different arrangements can obviously influence the torsional responses of the adjacent buildings. The layout which may results in severe eccentric poundings should be avoided in the design.

• The influence of setback on the pounding induced longitudinal and transverse displacements are not obvious. However, it significantly influences the torsional responses of the two adjacent buildings. Larger setback leads to larger torsional responses of two buildings but smaller pounding force between them.

• Separation gap will obviously influence the interactions between the adjacent buildings. Generally speaking, larger separation gap results in smaller pounding induced longitudinal, transverse displacements and rotational angle. Larger separation gap leads to less number of poundings but larger pounding force between two buildings.

It should be noted that the above conclusions are obtained based on the earthquake loadings shown in Fig. 4. To obtain more general conclusions, further studies are needed.

References

Anagnostopoulos, S.A. (1988), "Pounding of buildings in series during earthquakes", *Earthq. Eng. Struct. Dyn.*, **16**(3), 443-456.

Bi, K. and Hao, H. (2012), "Modelling and simulation of spatially varying earthquake ground motions at sites with varying conditions", *Probabilist. Eng. Mech.*, **29**, 92-104.

Bi, K. and Hao, H. (2013), "Numerical simulation of pounding damage to bridge structures under spatially varying ground motions", *Eng. Struct.*, **46**, 62-76.

Bi, K. and Hao, H. (2015), "Modelling of shear keys in bridge structures under seismic loads", *Soil Dyn. Earthq. Eng.*, **74**, 56-68.

Bi, K., Hao, H. and Chouw, N. (2013), "3D FEM analysis of pounding response of bridge structures at a canyon site to spatially varying ground motions", *Adv. Struct. Eng.*, **16**(4), 619-640.

Chau, K.T. and Wei, X.X. (2001), "Pounding of structures modelled as nonlinear impacts of two oscillators", *Earthq. Eng. Struct. Dyn.*, **30**(5), 633-651.

Chau, K.T., Wei, X.X., Guo, C. and Shen, C.Y. (2003), "Experimental and theoretical simulations of seismic poundings between adjacent structures", *Earthq. Eng. Struct. Dyn.*, **32**(4), 537-554.

Chouw, N. and Hao, H. (2012), "Pounding damage to buildings and bridges in the 22 February 2011 christchurch earthquake", *J. Protect. Struct.*, **3**(2), 123-139.

Cole, G., Dhakal, R., Carr, A. and Bull, D. (2011), "An investigation of the effects of mass distribution on pounding structures", *Earthq. Eng. Struct. Dyn.*, **40**(6), 641-659.

Cole, G.L., Dhakal, R.P. and Turner, F.M. (2012), "Building pounding damage observed in the 2011 christchurch

earthquake", *Earthq. Eng. Struct. Dyn.*, **41**(5), 893-913.

Davis, R.O. (1992), "Pounding of buildings modelled by an impact oscillator", *Earthq. Eng. Struct. Dyn.*, **21**(3) 253-274.

Efraimiadou, S., Hatzigeorgiou, G.D. and Beskos, D. (2013a), "Structural pounding between adjacent buildings subjected to strong ground motions. Part I: The effect of different structures arrangement", *Earthq. Eng. Struct. Dyn.*, **42**(10), 1509-1528.

Efraimiadou, S., Hatzigeorgiou, G.D. and Beskos, D. (2013b), "Structural pounding between adjacent buildings subjected to strong ground motions. Part II: The effect of multiple earthquakes", *Earthq. Eng. Struct. Dyn.*, **42**(10),1529-1545.

Favvata, M.J. (2017), "Minimum required separation gap for adjacent RC frames with potential inter-story seismic pounding", *Eng. Struct.*, **152**, 643-659.

Filiatrault, A., Cervantes, M., Folz, B. and Prion, H. (1994), "Pounding of buildings during earthquakes: A Canadian perspective", *Can. J. Civil Eng.*, **21**(2), 251-265.

Fiore, A., Marano, G.C. and Monaco, P (2013), "Earthquake-induced lateral-torsional pounding between two equal height multi-story buildings under multiple bi-directional ground motions", *Adv. Struct. Eng.*, **16**(5), 845-865.

Ghandil, M., and Aldaikh, H. (2017), "Damage-based seismic planar pounding analysis of adjacent symmetric buildings considering inelastic structure-soil-structure interaction", *Earthq. Eng. Struct. Dyn.*, **46**, 1141-1159.

Goldsmith, W. (1960), *Impact: The Theory and Physical Behavior of Colliding Solids*, Edward Arnold, London, U.K.

Gong, L. and Hao, H. (2005), "Analysis of coupled lateral-torsional-pounding responses of one-story asymmetric adjacent structures subjected to bi-directional ground motions. Part I: Uniform ground motion input", *Adv. Struct. Eng.*, **8**(5), 463-479.

Guo, A., Li, Z. and Li, H. (2011), "Point-to-surface pounding of highway bridges with deck rotation subjected to bi-directional earthquake excitations", *J. Earthq. Eng.*, **15**(2), 274-302.

Hao, H. (2015), "Analysis of seismic pounding between adjacent buildings", *Austr. J. Struct. Eng.*, **16**(3), 208-225.

Hao, H. and Gong, L. (2005), "Analysis of coupled lateral-torsional-pounding responses of one-story asymmetric adjacent structures subjected to bi-directional ground motions. Part II: Spatially varying ground motion input", *Adv. Struct. Eng.*, **8**(5), 481-495.

Hao, H., Bi, K., Chouw, N. and Ren, W.X. (2013), "State-of-the-art review on seismic induced pounding response of bridge structures", *J. Earthq. Tsunami*, **7**(3), 1350019.

Hao, H., Liu, X.Y. and Shen, J. (2000), "Pounding response of adjacent buildings subjected to spatial earthquake ground motions", *Adv. Struct. Eng.*, **3**(3), 145-162.

He, L., Shrestha, B., Hao, H., Bi, K. and Ren, W.X. (2017), "Experimental and three-dimensional finite element method studies on pounding responses of bridge structures subjected to spatially varying ground motions", *Adv. Struct. Eng.*, **20**, 105-124.

Jankowski, R. (2008), "Earthquake-induced pounding between equal height buildings with substantially different dynamic properties", *Eng. Struct.*, **30**(10), 2818-2829.

Jankowski, R. (2009), "Non-linear FEM analysis of earthquake-induced pounding between the main building and the stairway tower of the olive view hospital", *Eng. Struct.*, **31**(8), 1851-1864.

Jankowski, R. (2012), "Non-linear FEM analysis of pounding-involved response of buildings under non-uniform earthquake excitation", *Eng. Struct.*, **37**, 99-105.

Jing, H.S. and Young, M.H. (1991), "Impact interactions between two vibration systems under random excitation", *Earthq. Eng. Struct. Dyn.*, **20**(7), 667-681.

Leibovich, E., Rutenberg, A. and Yankelevsky, D.Z. (1996), "On

eccentric seismic pounding of symmetric buildings", *Earthq. Eng. Struct. Dyn.*, **25**(3), 219-233.

Mahmoud, S., Abd-Elhamed, A. and Jankowski R. (2013), "Earthquake-induced pounding between equal height multi-story buildings considering soil-structure interaction", *B. Earthq. Eng.*, **11**, 1021-1048.

Maison, B.F. and Kasai, K. (1990), "Analysis for the type of structural pounding", *J. Struct. Eng.*, **116**(4), 957-977.

Mouzakis, H.P. and Papadrakakis, M. (2004), "Three-dimensional nonlinear building pounding with friction during earthquakes", *J. Earthq. Eng.*, **8**(1), 107-132.

Papadrakakis, M., Apostolopoulou, C., Zacharopoulos, A. and Bitzarakis, S. (1996), "Three-dimensional simulation of structural pounding during earthquakes", *J. Eng. Mech.*, **122**(5), 423-431.

Polycarpou, P.C., Papaloizou, L. and Komofromos, P. (2014), "An efficient methodology for simulating earthquake-induced 3D pounding of buildings", *Earthq. Eng. Struct. Dyn.*, **43**(7), 985-1003.

Rajaram, C. and Ramancharla, P.K. (2012), "Three dimensional modelling of pounding between adjacent buildings", *Proceedings of the 4th International Conference on Structural Stability and Dynamics*, Jaipur, India, January.

Rosenblueth, E. and Meli, R. (1986), "The 1985 earthquake: Causes and effects in Mexico city", *Concrete Int.*, **8**(5), 23-34.

Soltysik, B. and Jankowski, R. (2016), *Earthquake-Induced Pounding between Asymmetric Steel Buildings in Seismic Behavior and Design of Irregular and Complex Civil Structures II*, Springer International Publishing, Switzerland.

Wang, L.X., Chau, K.T. and Wei, X.X. (2009), "Numerical simulations of nonlinear seismic torsional pounding between two single-story structures", *Adv. Struct. Eng.*, **12**(1), 87-101.

Zhu, P., Abe, S. and Fujino, Y. (2002), "Modelling of three-dimensional non-linear seismic performance of elevated bridges with emphasis on pounding of girders", *Earthq. Eng. Struct. Dyn.*, **31**(11), 591-609.

CC